Antiviral Research 88 (2010) 45–52

Contents lists available at ScienceDirect

Antiviral Research

journal homepage: www.elsevier.com/locate/antiviral

In vivo imaging assay for the convenient evaluation of antiviral compounds against cytomegalovirus in mice

Souichi Yamada[a], Isao Kosugi[b], Harutaka Katano[c], Yoshiko Fukui[a], Hideya Kawasaki[b], Yoshifumi Arai[b], Ichiro Kurane[a], Naoki Inoue[a,*]

[a] Department of Virology I, National Institute of Infectious Diseases, Tokyo, Japan
[b] Department of Pathology II, Hamamatsu University School of Medicine, Shizuoka, Japan
[c] Department of Pathology, National Institute of Infectious Diseases, Tokyo, Japan

ARTICLE INFO

Article history:
Received 31 December 2009
Received in revised form 29 June 2010
Accepted 6 July 2010

Keywords:
Mouse
Murine cytomegalovirus (MCMV)
In vivo imaging
Ganciclovir
Fluorescence
EGFP
DsRed2
1-(3,5-dichloro-4-pyridyl)piperidine-4-carboxamide
(DPPC)
Hairless

ABSTRACT

Evaluation of newly identified antiviral compounds against cytomegalovirus (CMV) in vivo still requires laborious and time-consuming experiments using a large number of animals. In this study, we examined an in vivo imaging assay for the evaluation of antiviral compounds using a recombinant murine CMV expressing EGFP (MCMV-GFP). We found the followings: (1) Fluorescent signals were detectable from 1 day after subcutaneous inoculation of the viruses into the backs of mice, and reached to the peak within 2–4 days. (2) Incubation period required for the signal appearance and peak signal intensities depended on the inoculated dose. (3) Not only BALB/c but also a hairless mouse strain, HR1, can be used for the assay, and no need to shave the HR1 mice added to the convenience of the assay. (4) However, BALB/c mice showed better sensitivity and dose–response to the inoculated virus, and inoculation with 200 PFUs of MCMV-GFP still yielded the signals. (5) Demonstration of the antiviral effect of ganciclovir provided a proof-of-concept. Thus, the in vivo imaging assay can allow the fast and convenient initial evaluation of anti-CMV candidate compounds in animals prior to comprehensive analyses.

1. Introduction

Human cytomegalovirus (HCMV) is the most common cause of congenital virus infection and is associated with significant morbidity in immunocompromised individuals, including transplant patients and other immunosuppressed patients (Pass, 2001). Currently available anti-HCMV drugs, such as ganciclovir (GCV) and foscarnet, can reduce the risk of CMV diseases and the mortality of transplant patients. GCV treatment can also reduce the risk of the progression of hearing loss in patients with symptomatic congenital CMV infection (Kimberlin et al., 2003). However, the side effects of GCV, such as neutropenia and thrombocytopenia, and development of resistant strains during long-term usage have necessitated the search for alternative compounds (Biron, 2006; Gilbert and Boivin, 2005). Several new types of therapeutic compounds have been under investigation (Biron, 2006; De Clercq, 2003; Visalli and van Zeijl, 2003), and some of the compounds, such as maribavir, have been evaluated in phase 2 and 3 clinical trials (Winston et al., 2008).

For the screening and evaluation of novel antiviral compounds in vitro, a plaque reduction assay has generally been used as standard assay. The slow growth of HCMV in tissue culture, however, makes the assay laborious and time-consuming, therefore, several modified high-throughput assays have been developed (for examples, Alexander et al., 2001; Bedard et al., 1999; Marschall et al., 2000; McSharry, 2000; Siennicka et al., 2002). Previously we established a reporter cell line for HCMV and identified some anti-HCMV compounds using this cell-based assay (Fukui et al., 2008).

Since CMV is species specific, animal models for the evaluation of antiviral agents have utilized surrogate animal viruses, including murine CMV (MCMV), rat CMV (RCMV) and guinea pig CMV (GPCMV) (reviewed in Kern, 2006). For the evaluation of anti-CMV compounds, intraperitoneal (i.p.) inoculation of normal mice with a lethal dose of MCMV has been widely used. Mice treated with cyclophosphamide and SCID mice infected with a lower dose of MCMV can be a model for immunosuppressed HIV-positive patients and transplant recipients (Weber et al., 2001; Duan et al., 1998). Since results based on MCMV/mice models may not be directly related to HCMV, SCID-hu mouse models in which human tissue is infected with HCMV have also been

* Corresponding author at: Department of Virology I, National Institute of Infectious Diseases, 1-23-1 Toyama, Shinjuku-ku, Tokyo 162-8640, Japan.
Tel.: +81 3 5285 1111; fax: +81 3 5285 1180.
E-mail address: ninoue@nih.go.jp (N. Inoue).

0166-3542/$ – see front matter © 2010 Elsevier B.V. All rights reserved.
doi:10.1016/j.antiviral.2010.07.002

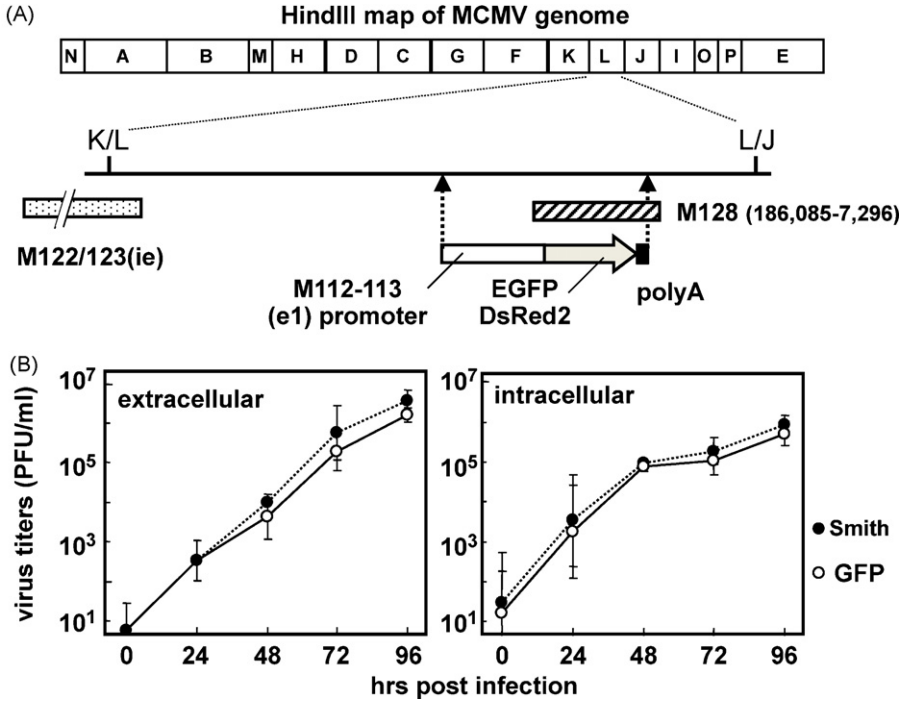

Fig. 1. (A) Construction of recombinant MCMVs. A schematic map of HindIII digests of the MCMV genome and the m128 gene region that was replaced with expression cassettes for fluorescent proteins, EGFP and DsRed2, respectively. (B) Comparison of growth capability in NIH3T3 cells between MCMV-GFP (open circles) and MCMV Smith strain (closed circles). Means and standard deviations (SD) of extra and intra-cellular virus titers are plotted.

developed (Bravo et al., 2007; Kern et al., 2004). However, the evaluation of new compounds in vivo based on survival rate of infected animals requires laborious and time-consuming experiments using a large number of animals. Otherwise we need to perform time-consuming histopathological detection of viral antigens, quantitative detection of viral DNA or titration of viruses in several types of organs of animals that were infected and then treated with compounds. Therefore, development of a faster alternative assay that requires fewer mice has been required. Recently, bioluminescence and fluorescence proteins have been used for the analysis of viral kinetics both in vitro and in vivo (reviewed in Luker and Luker, 2008). Recombinant vaccinia virus expressing luciferase-GFP fusion protein, for example, has been used for imaging in athymic nu/nu mice (Zaitseva et al., 2009). Although there have been a couple of publications describing in vivo imaging of mice infected with recombinant alphaherpesviruses, herpes simplex virus 1 (HSV-1) and varicella zoster virus (VZV), that express luciferase (Oliver et al., 2008; Luker et al., 2002), there has been no such application of this approach to the evaluation of anti-CMV compounds.

In this study, we made recombinant MCMVs expressing fluorescence proteins, and examined whether a fluorescence-based in vivo imaging assay was a faster alternative that requires fewer mice for semi-quantitative evaluation of anti-CMV compounds.

2. Materials and methods

2.1. Cells and viruses

NIH3T3 (ATCC CRL-1658) cells were propagated as described previously (Fukui et al., 2008). Mouse embryonic fibroblast (MEF) cells were prepared from ICR mice and were grown as reported previously (Tsutsui et al., 1995). MCMV Smith strain (ATCC VR-194) and recombinant MCMVs described below were propagated in MEF or NIH3T3 cells. Titration of virus stocks was performed by a standard plaque assay (Fukui et al., 2008).

pMCMVe1ProEGFP, a plasmid expressing EGFP under the control of the MCMV e1 promoter (e1Pro) (Arai et al., 2003), was constructed by replacing the HCMV enhancer/promoter region of pEGFP-C1 (Clontech, Mountain View, CA) with e1Pro. The upstream and downstream regions of the MCMV m128 gene, nucleotide positions 183,081–184,442 and 187,125–188,573, respectively, were amplified by PCR, and inserted into pMCMVe1ProEGFP to flank the EGFP expression cassette, resulting in pLR/MCMVe1ProEGFP. MCMV DNA was prepared as described previously (Straus et al., 1981), and cotransfected into MEF cells along with a DNA fragment spanning the upstream and downstream regions of the MCMV m128 gene and EGFP expression cassette of pLR/MCMVe1ProEGFP. MCMV expressing EGFP (MCMV-GFP) generated by homologous recombination in the cells was recovered, and isolated by three rounds of plaque purification (Fig. 1A). MCMV expressing DsRed2 (MCMV-DsRed2) was established in a similar way.

2.2. Chemicals

GCV (Wako Pure Chemical Industries, Japan) and 1-(3,5-dichloro-4-pyridyl) piperidine-4-carboxamide (DPPC) (Maybridge, UK) (Fukui et al., 2008) were dissolved in dimethylsulfoxide (DMSO) for use in this study.

2.3. Animal experiments

All animal procedures described below were approved by the Animal Care and Use Committee of the National Institute of Infectious Diseases (NIID), and were conducted according to 'the Guidelines for Animal Experiments Performed at the NIID'. Three-week-old female BALB/c inbred strain mice and four-week-old female HR1 closed colony mice used in this study were purchased from a commercial breeder (Japan SLC Inc.). Mice were infected subcutaneously with the indicated amount of plaque forming units (PFUs) of viruses followed by the daily intraperitoneal (i.p.) or

subcutaneous (s.c.) administration of antiviral compounds. For s.c. administration, antiviral compounds were injected within a few mm from the site of virus inoculation. Body weight and clinical signs for each mouse were recorded daily.

2.4. In vivo imaging and data analysis

The infected mice were anesthetized with 2% (v/v) isoflurane in air (Dainippon Sumitomo, Japan) using a MK-A100 device (Muromachi Kikai Co., Japan), and then positioned face down for in vivo imaging. In the case of BALB/c mice, the hair on their backs was shaved to decrease attenuation and scattering of transmitted light. Fluorescence signals from the mice were captured by an in vivo imaging device (Maestro, Cambridge Research & Instrumentation Inc., Woburn, MA), consisting of a CCD imaging sensor with a liquid crystal tunable filter (LCTF) and emission filter, an illumination module and a computer system for data analysis. Data capture was performed with a binning (resolution) factor of 2 and a 1.25 f/stop (aperture). All mice were placed in the same position to ensure the distance from their backs to the camera remained constant. Each image was converted into a pseudo-color illustration overlain on a gray-scale reference image of the whole mouse. The signal intensity for each mouse was calculated using Meta Imaging Software version 6.1 (Molecular Device) as the detected fluorescence emissions within a same-size area that was large enough to cover the positive areas in any mice.

2.5. Pathological examination

Skins obtained from sacrificed animals were fixed in 10% buffered formalin, embedded in paraffin, sectioned and finally stained with hematoxylin and eosin (HE), as described previously (Katano et al., 2007). Immunohistochemical analysis was performed with rat monoclonal antibody against MCMV ie1 (anti-IE1) or rat polyclonal antibody against MCMV ie3 (anti-IE3) as the primary antibody (Ishiwata et al., 2006). For the second and third phase immunostaining reagents, a biotinylated $F(ab')^2$ fragment of rabbit anti-rat immunoglobulin (DAKO) and peroxidase-conjugated streptavidin (DAKO) were used. 3,3′-diaminobenzidine (DAB) was used as a chromogen and the slides were counterstained with hematoxylin.

2.6. Statistical analysis

Correlation coefficient (r) between inoculation doses and fluorescence measurements was calculated by the Pearson product–moment correlation coefficient. Mann–Whitney U test was used to analyze statistical differences in fluorescence measurements between two groups of treatments. All comparisons were two-tailed.

3. Results

3.1. Growth of MCMV-GFP in vitro

In a one-step growth experiment, intra- and extra-cellular viral loads of the recombinant MCMV expressing EGFP (MCMV-GFP) were found to be similar to those of the parental strain MCMV Smith (Fig. 1B). Further, GCV and DPPC were shown to inhibit growth of MCMV-GFP as expected (Fukui et al., 2008).

3.2. In vivo imaging of hairless mice infected with MCMV-GFP

Hairless mice (HR1 strain), which are immunocompetent but genetically recessive homozygote for the *hairless* (*hr*) gene, and

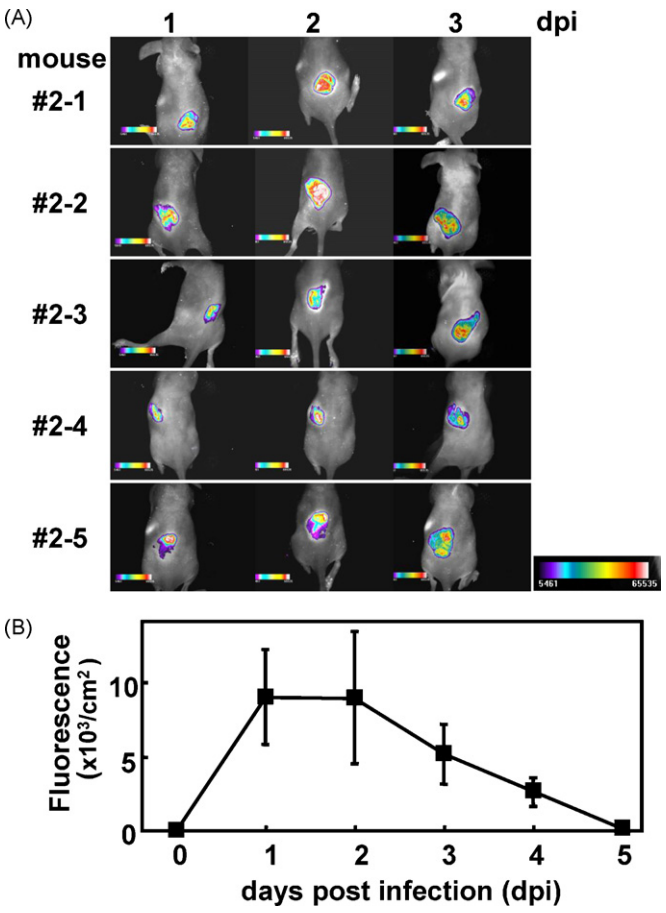

Fig. 2. In vivo imaging of HR1 mice infected with MCMV-GFP. (A) Five HR1 mice (#2-1 to #2-5) were subcutaneously infected with 1×10^5 PFUs of MCMV-GFP. Fluorescent images were captured daily from day 0 to day 5 after inoculation of virus. Day 0 means immediately after virus inoculation. Examples of the pseudo-colored images overlain on gray-scale photographs of mice are shown. The "rainbow-like" bars show relative intensities of fluorescence (from the weakest in violet to the strongest in red). (B) Means of fluorescence per cm^2 obtained from the five mice shown in the panel A are plotted. Error bars represent the standard deviations (SD).

BALB/c mice subcutaneously infected with 2×10^6 PFUs of recombinant MCMVs did show neither any decrease in body weight nor clinical symptoms and death during the observation period up to 7 days post-infection (dpi).

First, we examined the feasibility of in vivo imaging using five hairless mice (HR1 strain). The signals from the animals infected with 1×10^5 PFUs of MCMV-GFP were quantified and expressed as fluorescence per cm^2. As shown in Fig. 2, fluorescent signals were apparent from 1 dpi, reached to a maximum at 2 dpi, and then decreased gradually. In HR1 mice, however, fluorescence signals were only detectable when they were infected with more than 1×10^4 PFU of MCMV-GFP, and there was no apparent dose response between 1×10^4 PFU to 1×10^6 PFU (data not shown).

3.3. In vivo imaging of BALB/c mice infected with MCMV-GFP

We next used BALB/c mice, since the HR1 strain is derived from CBA mice that were reported to be a MCMV-infection resistant strain. BALB/c mice were infected subcutaneously with 10-fold serial dilutions of MCMV-GFP from 200 PFUs to 2×10^6 PFUs per mouse (seven mice per condition). Fluorescence signals were detected from the mice infected with more than 200 PFUs of MCMV-GFP (Fig. 3). The initial appearance of the signals was

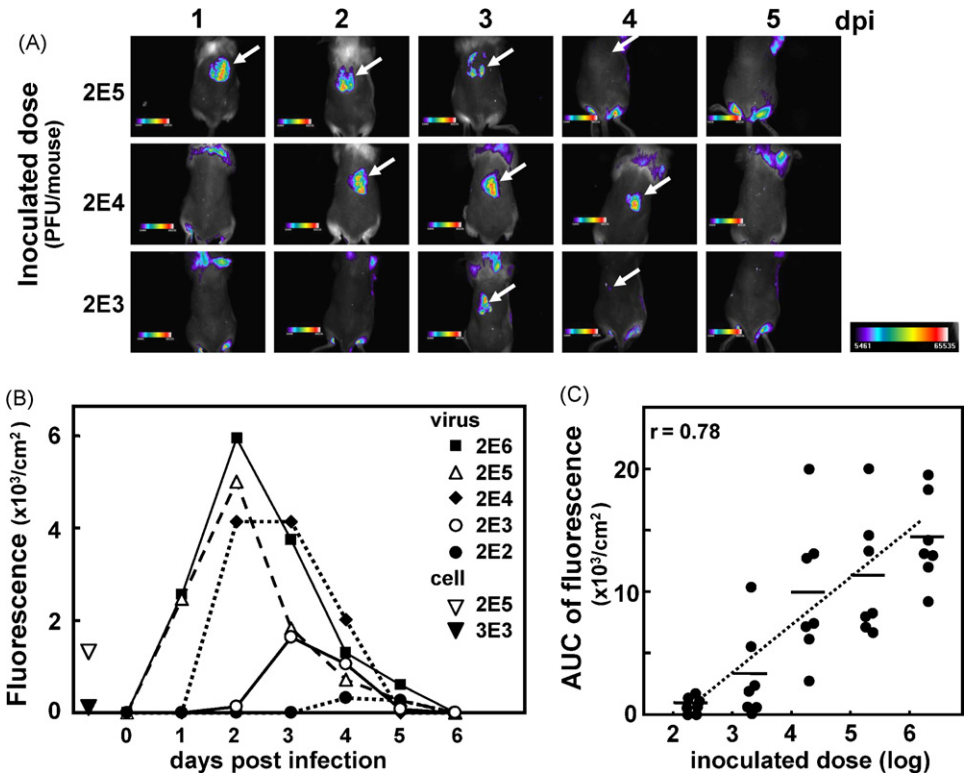

Fig. 3. In vivo imaging of BALB/c mice infected with MCMV-GFP. (A) BALB/c mice were subcutaneously infected with 2×10^2 (2E2) to 2×10^6 (2E6) PFUs of MCMV-GFP, and fluorescent signals were captured daily. Seven mice were used for each set of conditions. Examples of images of the mice infected with 2×10^3 to 2×10^5 of MCMV-GFP are shown. Non-specific signals around the edge of each body are due to hairs remaining after shaving. Arrows indicate specific GFP-derived signals. (B) Means of fluorescence per cm^2 obtained from the seven mice at the indicated day post-infection (dpi) are plotted for each set of conditions. To compare with the signals from the virus infection, 3×10^3 (closed arrow) and 2×10^5 (open arrow) cells infected with MCMV-GFP were inoculated into the back of mice, and their images were captured within 1 h. (C) Area under curve (AUC) of fluorescence for each mouse against inoculated virus dose for the mouse is plotted. Each dot represents one mouse. Horizontal bars show means of the AUC for each condition.

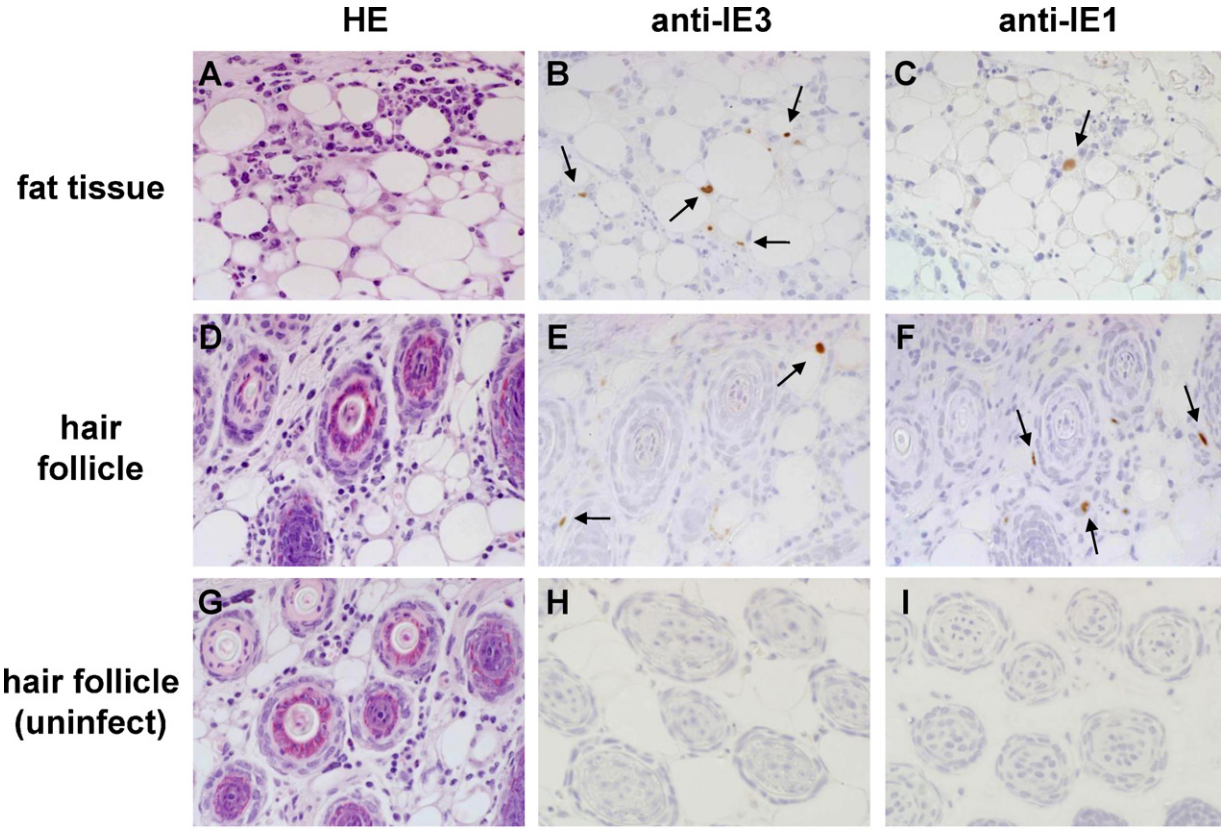

Fig. 4. Pathological examination of the skins of the BALB/c mice uninfected (G–I) and infected with MCMV-GFP (A–F). HE staining and immunohistochemical (IHC) staining with antibodies against MCMV ie1 (IE1) and ie3 (IE3) are shown for skin fat tissue and hair follicles. Arrows indicate positive signals.

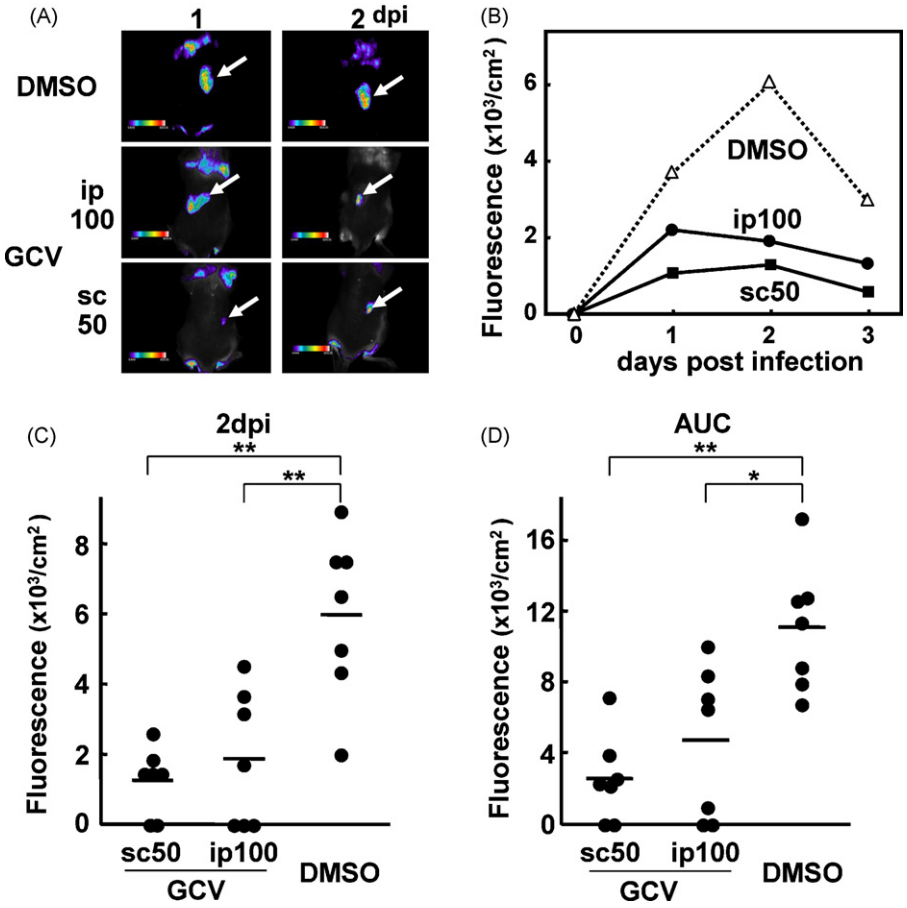

Fig. 5. In vivo imaging assay for the evaluation of antiviral effects of GCV. BALB/c mice were subcutaneously infected with 1×10^5 PFUs of MCMV-GFP, then GCV was administrated daily from 6 h post-infection (p.i.) under the following conditions: i.p., 100 mg/kg/dose (ip100), and s.c., 50 mg/kg/dose (sc50). As a control, DMSO used as solvent for GCV was administrated. Seven mice were used for each set of condition. (A) Pseudo-colored images overlain on gray-scale photographs of mice at 1 and 2 dpi (one mice per condition) are shown. To distinguish from non-specific signals, the regions with EGFP fluorescence in BALB/c mice are shown with arrows. (B) Means of fluorescence per cm^2 obtained from the seven mice at the indicated dpi are plotted. (C and D) Fluorescence at 2 dpi (C) and AUC of fluorescence (D) obtained from each mouse is plotted. Each closed circle means one mouse. Horizontal bars are means of the signals. $^*p < 0.05$ and $^{**}p < 0.01$.

dose-dependent (Fig. 3B); for example, 1 dpi in the mice with $>2 \times 10^5$ PFU, 2 dpi with 2×10^4 PFU, 3 dpi with 2×10^3 PFU and 4 dpi with 2×10^2 PFU. By 5 or 6 dpi, the fluorescent signals disappeared from almost all of the mice. The area under curve (AUC) of fluorescence signals from day 0 to day 6 was obtained for each animal, and compared with its inoculated virus dose. A correlation ($r = 0.78$) that may allow semi-quantitative use of the assay was observed between those two parameters (Fig. 3C). To estimate the numbers of lytically infected cells in the mice, 3×10^3 and 2×10^5 cells infected with MCMV-GFP were inoculated into the back of mice, and their images were captured within 1hr. The signal intensity from the 2×10^5 cells was almost equivalent to the peak value for mice infected with 2×10^3 PFUs, indicating a more than 100-fold increase of MCMV-GFP- infected cells within a couple of days (Fig. 3B).

3.4. Confirmation of viral antigens in the areas detected by in vivo imaging assay

Immunohistochemical examination with antibodies specific to MCMV ie1 and ie3 antigens demonstrated that viral antigen-positive cells were distributed around hair follicles and in subcutaneous fat tissue (Fig. 4). The viral antigens were detected in these areas in all mice with fluorescent signals, indicating that the in vivo imaging assay detected cells infected with MCMV-GFP but not GFP that had leaked from the infected cells.

3.5. Evaluation of antiviral compounds

As a proof-of-concept, the effects of GCV on the growth of MCMV-GFP in BALB/c mice were evaluated by the in vivo imaging assay. Seven mice were used for each condition. As shown in Fig. 5A and B, i.p. administration of 100 mg/kg/dose and s.c. administration of 50 mg/kg/dose of GCV decreased the fluorescent signals, indicating inhibition of viral growth. In contrast, i.p. administration of 50 mg/kg/dose of GCV did not reduce the signals (data not shown). Comparison of the signal intensities at the 2 dpi point as well as that of AUC intensities among the conditions indicates statistical significances (Fig. 5C and D).

Next, DPPC, which was previously identified as a new type of antiviral compounds in our in vitro assay, was evaluated in BALB/c mice. Although i.p. administration of DPPC did not decrease fluorescent signals at all (data not shown), subcutaneous administration of 50 mg/kg/dose delayed the appearance of the signals and decreased the signal intensity (Fig. 6). Although no systematical analysis was undertaken, administrations of 100 mg/kg/dose of DPPC seemed to be slightly toxic to the mice. In a preliminary experiment using HR1 mice, similar results were observed (data not shown).

4. Discussion

In this study, we established an in vivo imaging assay for the evaluation of compounds against CMV in animals. The advantages

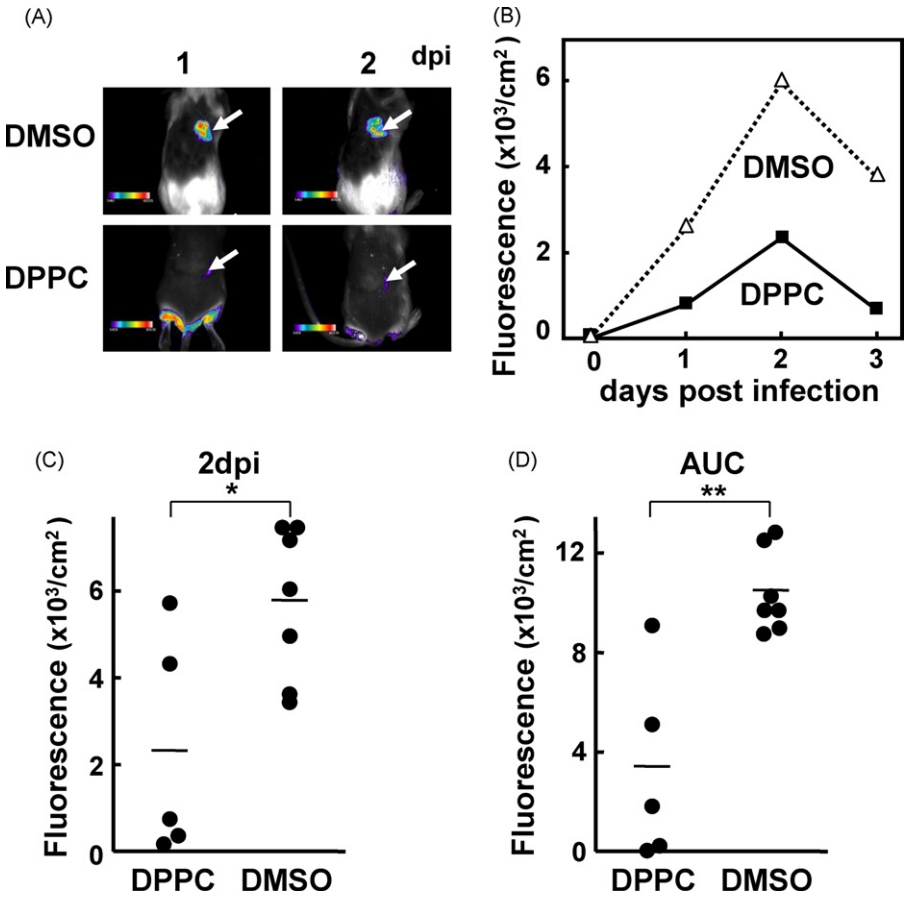

Fig. 6. In vivo imaging assay for the evaluation of DPPC. BALB/c mice were infected with MCMV-GFP, and 50 mg/kg/dose of DPPC and DMSO were subcutaneously administrated daily from 1 h p.i. (A) Examples of pseudo-colored images overlain on gray-scale photographs of the mice at 1 and 2 dpi are shown. Arrows indicate EGFP-specific signals. (B) Means of fluorescence obtained from the seven mice treated with DMSO (open triangles) and the five mice treated with DPPC (closed squares) are plotted. (C and D) Fluorescence at 2 dpi (C) and AUC of the fluorescence (D) obtained from each mouse is plotted. Each closed circle means one mouse. Horizontal bars indicate means of the signals. $^{*}p < 0.05$ and $^{**}p < 0.01$.

of this assay include (i) evaluation of compounds for antiviral activities within a few days, which is faster than the conventional methods, (ii) use of a minimum number of mice, and (iii) no need of immunohistochemical analysis. The limitations of the assay are as follows: (i) it requires an imaging device, (ii) it gives only semi-quantitative evaluation, (iii) loss of fluorescence, for example, degradation or inhibition of GFP by test compounds, may result in false interpretation of effectiveness of the compounds, and (iv) as discussed later, s.c. inoculation as well as s.c. administration of compounds may not reflect the true "in vivo" situation, making comparison of the outcomes with those obtained by the traditional methods difficult. Although our assay has those limitations and does not provide comprehensive evaluation of each compound, easy elimination of compounds that show antiviral activities in vitro but not in vivo by the assay allow high-throughput selection of better candidate compounds for further study without sacrificing many animals.

Bioluminescence and fluorescence is very useful for non-invasive imaging studies. Several studies have already demonstrated the usefulness of fluorescence-based antiviral assays for the evaluation of compounds in vitro (Dal Pozzo et al., 2008). Since bioluminescence is generated by the reaction of luciferase with its substrate, experiments using bioluminescence imaging need a standardized protocol, including the amount of substrate, the delay between injection and imaging, and the positioning of the mice (Luker and Luker, 2008). In contrast, fluorescence-based assays have a limitation in quantitative analyses. A couple of factors, including the attenuation of light by hair and organ pigmentation, depth from the surface, and wave length of fluorescence, may affect the outcomes of in vivo imaging based on fluorescence. For example, in this study, we compared the outcomes for fluorescent proteins, EGFP and DsRed2, using identical recombinant viruses except for the expressing fluorescent proteins. Signals from mice infected with MCMV-DsRed were significantly lower than those with MCMV-GFP (data not shown), probably because DsRed2 but not EGFP requires oligomerization to become active, as the result, higher concentration in infected cells. We also compared mouse strains, BALB/c and HR1. The advantages and disadvantages of those strains for in vivo imaging are as follows. BALB/c requires clipping and shaving of the hair of the back each time before imaging, and some non-specific signals from remaining hairs were still observed. In addition, the initial appearance of the signals in HR1 mice was earlier than in BALB/c mice, probably due to the thinner skin in HR1. However, the minimum dose for positive signals in BALB/c mice was about 50-fold smaller than that in HR1 mice and the fluorescent signals in the BALB/c mice were more dose-dependent. Based on the growth capacity of MCMV, mouse strains have been classified as susceptible (BALB/c), moderately resistant (C57BL/6) and resistant (CBA) (Allan and Shellam, 1984). The resistance is not absolute and the difference in MCMV yields is approximately 20-fold between BALB/c and CBA mice (Smith et al., 2008). This resistance may reflect a higher dose requirement for HR1 mice for in vivo imaging.

The major factor that made our in vivo imaging assay practical is the s.c. inoculation with MCMV-GFP, which allows easy semi-

quantitative measurement of the signals in BALB/c mice. Although we tried i.p. inoculation, it was difficult to capture signals consistently. One drawback of s.c. inoculation is the fact that the way in which viruses disseminate after inoculation and the types of cells initially infected are not well defined. Very recently, Hsu et al. (2009) analyzed cell types infected with MCMV expressing GFP in C57BL/6 mice after i.p. inoculation, and found that MCMV traffics as free virus from the peritoneal cavity to the mediastinal lymphatics. Sacher et al. (2008) developed MCMV expressing GFP in a cell type-specific way, and demonstrated that intravenous (i.v.) and i.p. inoculation resulted in the productive infection of endothelial cells in most organs followed by a spreading to neighboring cells within the organ and in blood vessels. Although the biological relevance of s.c. inoculation to human diseases is unclear, we do not intend to develop the assay for comprehensive analyses that can be applied to human situations. Rather, we would like to speed up the process for initial in vivo evaluation.

We demonstrated the usefulness of our in vivo imaging assay for the evaluation of antiviral compounds by the i.p. and s.c. administration of GCV. The effective doses in our assay were similar to those described in previous reports (Duan et al., 1998; Reefschlaeger et al., 2001; Braitman et al., 1991). We also applied the assay to the evaluation of DPPC, a compound identified by in vitro screening (Fukui et al., 2008). Subcutaneous administration of DPPC decreased the fluorescent signals. Such s.c. administration is almost like an in vitro experiment on the back of a mouse and may not be an accepted procedure to observe true in vivo effects of compounds. However, since CMV can infect various cell types in vitro and in vivo, the s.c. administration procedure may serve as an assay positioning between the true traditional in vivo assay and the usual in vitro assay in a particular cell type, for example in fibroblast cells. Since the pharmacokinetics of DPPC in mice is not known, if DPPC has a shorter half-life or a smaller bioavailability than GCV, the effectiveness of DPPC might be underestimated. Thus, this study warrants further comprehensive studies on DPPC, including pharmacokinetical studies, the traditional survival experiments and in vivo imaging in the SCID-hu model.

In conclusion, we demonstrated that in vivo imaging assay is useful technique for the fast screening and evaluation of antiviral compounds prior to large-scale and meticulous animal studies.

Acknowledgements

We thank Phil Pellett for his intellectual input, Keiko Yashiro and Saki Fukuchi for their technical assistance, and Minoru Tobiume for statistical analysis of in vivo imaging. This work was supported by a Grant for Research Promotion of Emerging and Re-emerging Infectious Diseases from the Ministry of Health, Labor and Welfare, Japan (H21-Shinko-Ippan-009), to Katano and Inoue.

References

Alexander, R., Lamb, D., White, D., Wentzel, T., Politis, S., Rijnsburger, J., van Ruyven, D., Kelly, N., Garland, S.M., 2001. 'RETCIF': a rapid, sensitive method for detection of viruses, applicable for large numbers of clinical samples. J. Virol. Meth. 97, 77–85.

Allan, J.E., Shellam, G.R., 1984. Genetic control of murine cytomegalovirus infection: virus titres in resistant and susceptible strains of mice. Arch. Virol. 81, 139–150.

Arai, Y., Ishiwata, M., Baba, S., Kawasaki, H., Kosugi, I., Li, R.Y., Tsuchida, T., Miura, K., Tsutsui, Y., 2003. Neuron-specific activation of murine cytomegalovirus early gene e1 promoter in transgenic mice. Am. J. Pathol. 163, 643–652.

Bedard, J., May, S., Barbeau, D., Yuen, L., Rando, R.F., Bowlin, T.L., 1999. A high throughput colorimetric cell proliferation assay for the identification of human cytomegalovirus inhibitors. Antiviral Res. 41, 35–43.

Biron, K.K., 2006. Antiviral drugs for cytomegalovirus diseases. Antiviral Res. 71, 154–163.

Braitman, A., Swerdel, M.R., Olsen, S.J., Tuomari, A.V., Lynch, J.S., Blue, B., Michalik, T., Field, A.K., Bonner, D.P., Clark, J.M., 1991. Evaluation of SQ 34,514: pharmacokinetics and efficacy in experimental herpesvirus infections in mice. Antimicrob. Agents Chemother. 35, 1464–1468.

Bravo, F.J., Cardin, R.D., Bernstein, D.I., 2007. A model of human cytomegalovirus infection in severe combined immunodeficient mice. Antiviral Res. 76, 104–110.

Dal Pozzo, F., Andrei, G., Daelemans, D., Winkler, M., Piette, J., De Clercq, E., Snoeck, R., 2008. Fluorescence-based antiviral assay for the evaluation of compounds against vaccinia virus, varicella zoster virus and human cytomegalovirus. J. Virol. Meth. 151, 66–73.

De Clercq, E., 2003. New inhibitors of human cytomegalovirus (HCMV) on the horizon. J. Antimicrob. Chemother. 51, 1079–1083.

Duan, J., Paris, W., Kibler, P., Bousquet, C., Liuzzi, M., Cordingley, M.G., 1998. Dose and duration-dependence of ganciclovir treatment against murine cytomegalovirus infection in severe combined immunodeficient mice. Antiviral Res. 39, 189–197.

Fukui, Y., Shindoh, K., Yamamoto, Y., Koyano, S., Kosugi, I., Yamaguchi, T., Kurane, I., Inoue, N., 2008. Establishment of a cell-based assay for screening of compounds inhibiting very early events in the cytomegalovirus replication cycle and characterization of a compound identified using the assay. Antimicrob. Agents Chemother. 52, 2420–2427.

Gilbert, C., Boivin, G., 2005. New reporter cell line to evaluate the sequential emergence of multiple human cytomegalovirus mutations during in vitro drug exposure. Antimicrob. Agents Chemother. 49, 4860–4866.

Hsu, K.M., Pratt, J.R., Akers, W.J., Achilefu, S.I., Yokoyama, W.M., 2009. Murine cytomegalovirus displays selective infection of cells within hours after systemic administration. J. Gen. Virol. 90, 33–43.

Ishiwata, M., Baba, S., Kawashima, M., Kosugi, I., Kawasaki, H., Kaneta, M., Tsuchida, T., Kozuma, S., Tsutsui, Y., 2006. Differential expression of the immediate-early 2 and 3 proteins in developing mouse brains infected with murine cytomegalovirus. Arch. Virol. 151, 2181–2196.

Katano, H., Sato, Y., Tsutsui, Y., Sata, T., Maeda, A., Nozawa, N., Inoue, N., Nomura, Y., Kurata, T., 2007. Pathogenesis of cytomegalovirus-associated labyrinthitis in a guinea pig model. Microbes Infect. 9, 183–191.

Kern, E.R., 2006. Pivotal role of animal models in the development of new therapies for cytomegalovirus infections. Antiviral Res. 71, 164–171.

Kern, E.R., Bidanset, D.J., Hartline, C.B., Yan, Z., Zemlicka, J., Quenelle, D.C., 2004. Oral activity of a methylenecyclopropane analog, cyclopropavir, in animal models for cytomegalovirus infections. Antimicrob. Agents Chemother. 48, 4745–4753.

Kimberlin, D.W., Lin, C.Y., Sanchez, P.J., Demmler, G.J., Dankner, W., Shelton, M., Jacobs, R.F., Vaudry, W., Pass, R.F., Kiell, J.M., Soong, S.J., Whitley, R.J., 2003. Effect of ganciclovir therapy on hearing in symptomatic congenital cytomegalovirus disease involving the central nervous system: a randomized, controlled trial. J Pediatr. 143, 16–25.

Luker, G.D., Bardill, J.P., Prior, J.L., Pica, C.M., Piwnica-Worms, D., Leib, D.A., 2002. Noninvasive bioluminescence imaging of herpes simplex virus type 1 infection and therapy in living mice. J. Virol. 76, 12149–12161.

Luker, K.E., Luker, G.D., 2008. Applications of bioluminescence imaging to antiviral research and therapy: multiple luciferase enzymes and quantitation. Antiviral Res. 78, 179–187.

Marschall, M., Freitag, M., Weiler, S., Sorg, G., Stamminger, T., 2000. Recombinant green fluorescent protein-expressing human cytomegalovirus as a tool for screening antiviral agents. Antimicrob. Agents Chemother. 44, 1588–1597.

McSharry, J.J., 2000. Analysis of virus-infected cells by flow cytometry. Methods 21, 249–257.

Oliver, S.L., Zerboni, L., Sommer, M., Rajamani, J., Arvin, A.M., 2008. Development of recombinant varicella-zoster viruses expressing luciferase fusion proteins for live in vivo imaging in human skin and dorsal root ganglia xenografts. J. Virol. Methods 154, 182–193.

Pass, R.F., 2001. Cytomegalovirus. In: Knipe, D.M., Howley, P.M. (Eds.), Fields Virology, 4th ed. Lippincott Williams & Wilkins, Philadelphia, PA, pp. 2675–2705.

Reefschlaeger, J., Bender, W., Hallenberger, S., Weber, O., Eckenberg, P., Goldmann, S., Haerter, M., Buerger, I., Trappe, J., Herrington, J.A., Haebich, D., Ruebsamen-Waigmann, H., 2001. Novel non-nucleoside inhibitors of cytomegaloviruses (BAY 38-4766): in vitro and in vivo antiviral activity and mechanism of action. J. Antimicrob. Chemother. 48, 757–767.

Sacher, T., Podlech, J., Mohr, C.A., Jordan, S., Ruzsics, Z., Reddehase, M.J., Koszinowski, U.H., 2008. The major virus-producing cell type during murine cytomegalovirus infection, the hepatocyte, is not the source of virus dissemination in the host. Cell Host. Microbe 3, 263–272.

Siennicka, J., Trzcinska, A., Kantoch, M., 2002. Evaluation of antiviral activity of different origin compounds by flow cytometry. Acta Microbiol. Pol. 51, 79–83.

Smith, L.M., McWhorter, A.R., Masters, L.L., Shellam, G.R., Redwood, A.J., 2008. Laboratory strains of murine cytomegalovirus are genetically similar to but phenotypically distinct from wild strains of virus. J. Virol. 82, 6689–6696.

Straus, S.E., Aulakh, H.S., Ruyechan, W.T., Hay, J., Casey, T.A., Vande Woude, G.F., Owens, J., Smith, H.A., 1981. Structure of varicella-zoster virus DNA. J. Virol. 40, 516–525.

Tsutsui, Y., Kashiwai, A., Kawamura, N., Aiba-Masago, S., Kosugi, I., 1995. Prolonged infection of mouse brain neurons with murine cytomegalovirus after pre- and perinatal infection. Arch. Virol. 140, 1725–1736.

Visalli, R.J., van Zeijl, M., 2003. DNA encapsidation as a target for anti-herpesvirus drug therapy. Antiviral Res. 59, 73–87.
Weber, O., Bender, W., Eckenberg, P., Goldmann, S., Haerter, M., Hallenberger, S., Henninger, K., Reefschlager, J., Trappe, J., Witt-Laido, A., Ruebsamen-Waigmann, H., 2001. Inhibition of murine cytomegalovirus and human cytomegalovirus by a novel non-nucleosidic compound in vivo. Antiviral Res. 49, 179–189.
Winston, D.J., Young, J.A., Pullarkat, V., Papanicolaou, G.A., Vij, R., Vance, E., Alangaden, G.J., Chemaly, R.F., Petersen, F., Chao, N., Klein, J., Sprague, K., Villano, S.A., Boeckh, M., 2008. Maribavir prophylaxis for prevention of cytomegalovirus infection in allogeneic stem cell transplant recipients: a multicenter, randomized, double-blind, placebo-controlled, dose-ranging study. Blood 111, 5403–5410.
Zaitseva, M., Kapnick, S.M., Scott, J., King, L.R., Manischewitz, J., Sirota, L., Kodihalli, S., Golding, H., 2009. Application of bioluminescence imaging to the prediction of lethality in vaccinia virus-infected mice. J. Virol. 83, 10437–10447.